Supplementary information

Lanthanide(III) complexes of monophosphinate/monophosphonate DOTA-analogues: effect of the substituents on formation rate and radiolabelling yield

Soňa Procházková,[a] Vojtěch Kubíček,[a]* Jan Kotek,[a] Adrienn Vágner,[b] Johannes Notni[b] and Petr Hermann[a]

[a] Department of Inorganic Chemistry, Faculty of Science, Charles University, Hlavova 2030, 128 43 Prague 2, Czech Republic; email: kubicek@natur.cuni.cz; tel.: +420 221951436; fax: +420 221951253.

[b] Lehrstuhl für Pharmazeutische Radiochemie, Technische Universität München, Walther-Meissner-Strasse 3, D-85748 Garching, Germany.

Table of content

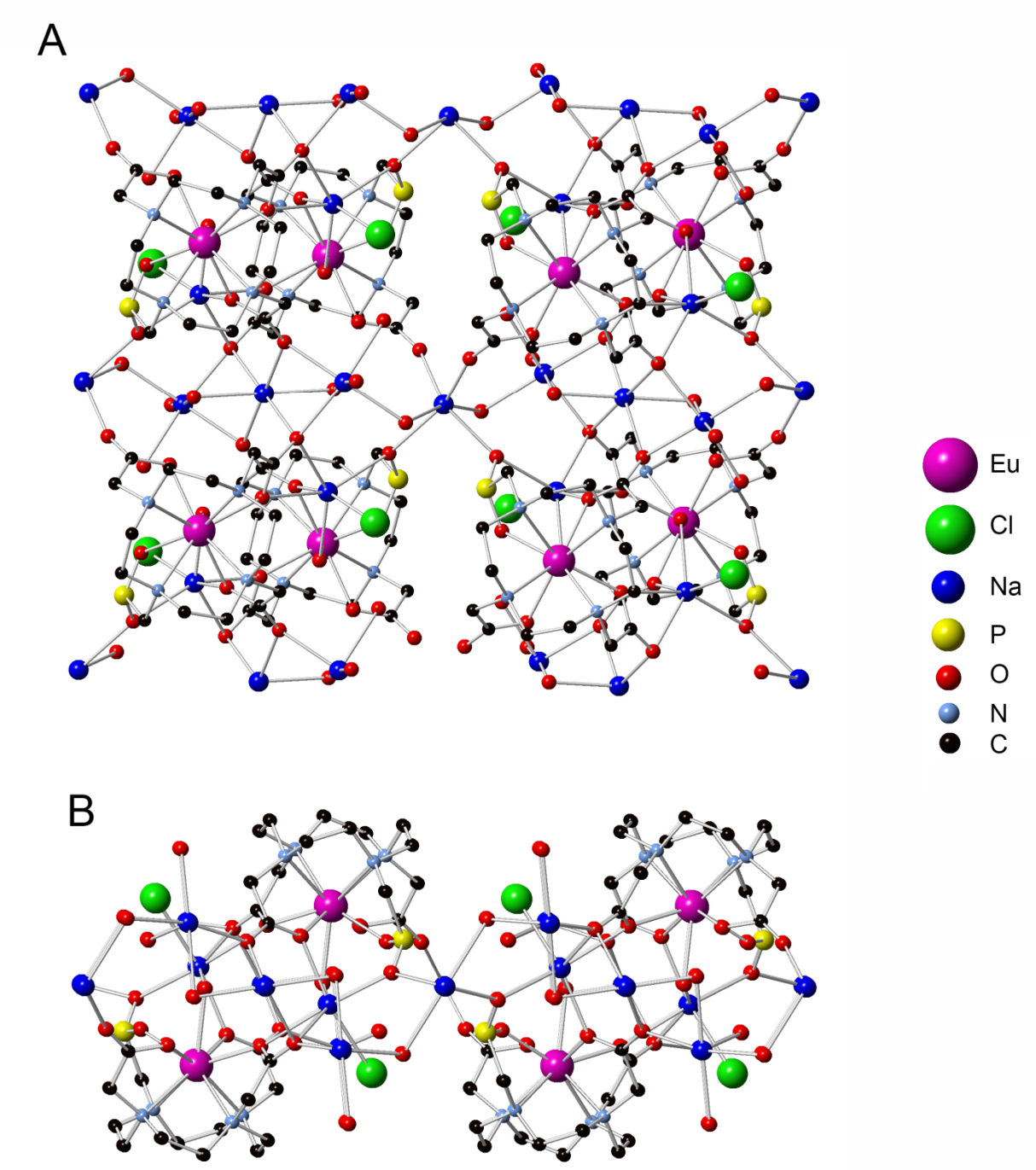

Figure S1. 2D coordination polymer motive found in the solid-state structure of $Na[Eu(do3aP^{H})(H_2O)]\cdot 2NaCl\cdot 7.125H_2O$. The view perpendicular to O_4/N_4-planes of the coordination spheres (**A**) and the view along the *y*-axis (**B**). Hydrogen atoms are omitted for clarity.

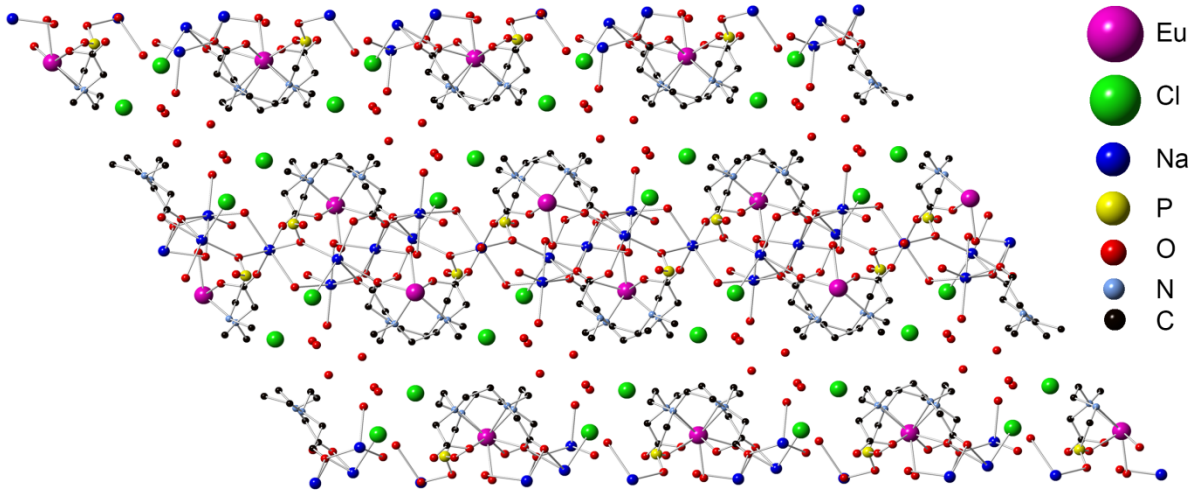

Figure S2. Crystal packing of Na[Eu(do3aP^{H})(H_2O)]·2NaCl·7.125H_2O. The view along the *y*-axis. Hydrogen atoms are omitted for clarity.

Isolation and structure of DO3A lactame – H_2do3a^{lac}

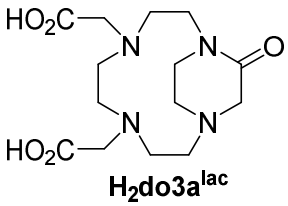

H_2do3a^{lac}

When old batches of H_3do3a were used for synthesis of H_4do3aP^H (especially when stored in semi-solid form obtained by evaporation from acid media after deesterification), some amount of lactam H_2do3a^{lac} was isolated as a late fraction of the ion exchange workup of the reaction mixture. It is probably predominantly formed on pro-longed standing of H_3do3a under acid conditions (after evaporation in CF_3COOH). Its ^1H NMR spectra are rather complicated due to rigidity of the molecule and, thus, the X-ray diffraction study was performed to confirm identity of the compound (Figure S3).

Single-crystals of $(H_4do3a^{lac})Cl_2\cdot 2H_2O$ were grown by vapour diffusion of THF into the solution of the H_4do3a^{lac} in 6 M aq. HCl. In the crystal structure of $(H_4do3a^{lac})Cl_2\cdot 2H_2O$, no disorder was found. The thermal parameter of one water-belonging hydrogen atoms was kept using $U_{eq}(H) = 1.2\ U_{eq}(O)$ as it became too large when freely refined.

The macrocycle of $(H_4do3a^{lac})^{2+}$ fragment is diprotonated. One of the protons is bound to the amine atom of the lactam ring, and the other is localized on the opposite nitrogen atom bearing one of the carboxylate pendants and is involved in the medium-strong intramolecular hydrogen bond ($d_{N\cdots O}$ = 2.88 Å) to the lactam oxygen atom. Both carboxylic acid pendant arms are protonated and involved in intermolecular hydrogen bonding with water molecules of crystallization and chloride counter anions.

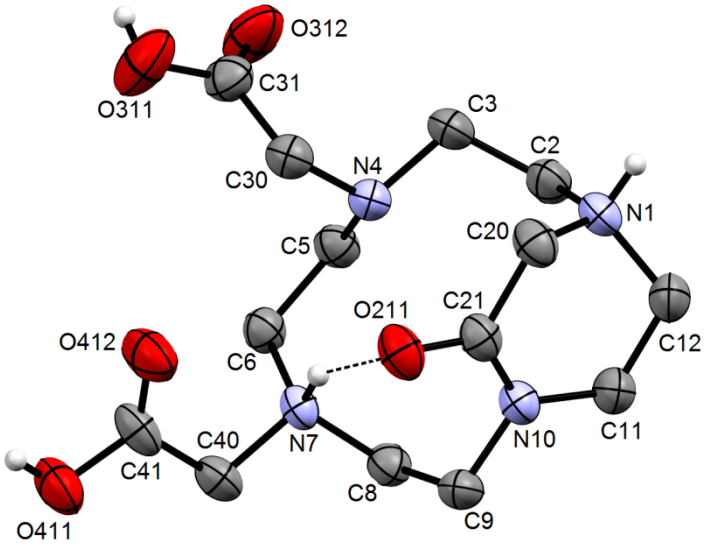

Figure S3. Molecular structure of $(H_4do3a^{lac})^{2+}$ cation found in the crystal structure of $(H_4do3a^{lac})Cl_2\cdot 2H_2O$. The intramolecular hydrogen bond is shown as a dashed line. Carbon-bound hydrogen atoms are omitted for clarity.

Table S1. Experimental data of the reported crystal structures.

Compound	$(H_6do3aP^H)Cl_2 \cdot THF \cdot 3H_2O$	$Na[Eu(do3aP^H)(H_2O)] \cdot 2NaCl \cdot 7.125H_2O$	$(H_4do3a^{lam})Cl_2 \cdot 2H_2O$
Formula	$C_{19}H_{45}N_4O_{12}P_1Cl_2$	$C_{15}H_{41.25}Cl_2Eu_1N_4Na_3O_{16.125}P_1$	$C_{14}H_{30}Cl_2N_4O_7$
M_r	623.46	858.57	437.32
Colour	colourless	colourless	colourless
Shape	prism	needle	prism
Dimensions (mm)	0.30×0.25×0.20	0.15×0.08×0.05	0.50×0.20×0.20
Crystal system	monoclinic	monoclinic	orthorhombic
Space group	C2/*c*	C2/*c*	$P2_12_12_1$
a (Å)	22.0543(3)	32.1447(5)	9.7430(4)
b (Å)	11.19790(10)	9.43790(10)	10.3130(5)
c (Å)	24.5815(4)	23.5537(4)	21.7340(10)
α (°)	90	90	90
β (°)	96.4613(8)	121.0061(8)	90
γ (°)	90	90	90
V (Å^3)	6032.13(14)	6124.65(16)	2183.82(17)
Z	8	8	4
D_c (g cm^{-3})	1.373	1.862	1.330
μ (mm^{-1})	0.329	2.392	0.337
F(000)	2656	3466	928
Reflections unique; observed ($I_o > 2\sigma(I)$)	6889; 5601	7035; 6005	4220; 3435
Parameters	432	451	276
G-o-f on F^2	1.078	1.039	1.066
R; *R*' (all data)	0.0466; 0.0650	0.0299; 0.0406	0.0439; 0.0620
wR; *wR*' (all data)	0.1291; 0.1449	0.0658; 0.0709	0.0987; 0.1088
Difference max; min (e Å^{-3})	0.474; –0.523	1.941; –1.169	0.321; –0.181

Table S2. Overall protonation constants logβ of ligands (I = 0.1 M NMe_4Cl, 25 °C).

	H_4do3aP^H	H_5do3aP^{PIN}	H_4do3aP^{AM}
HL	12.43(1)	12.46(1)	13.29(3)
H_2L	21.53(1)	21.86(2)	22.85(3)
H_3L	25.86(1)	26.41(2)	31.30(3)
H_4L	28.64(1)	29.83(2)	35.41(3)
H_5L	30.09(1)	31.89(2)	37.27(3)
H_6L	–	–	38.25(4)

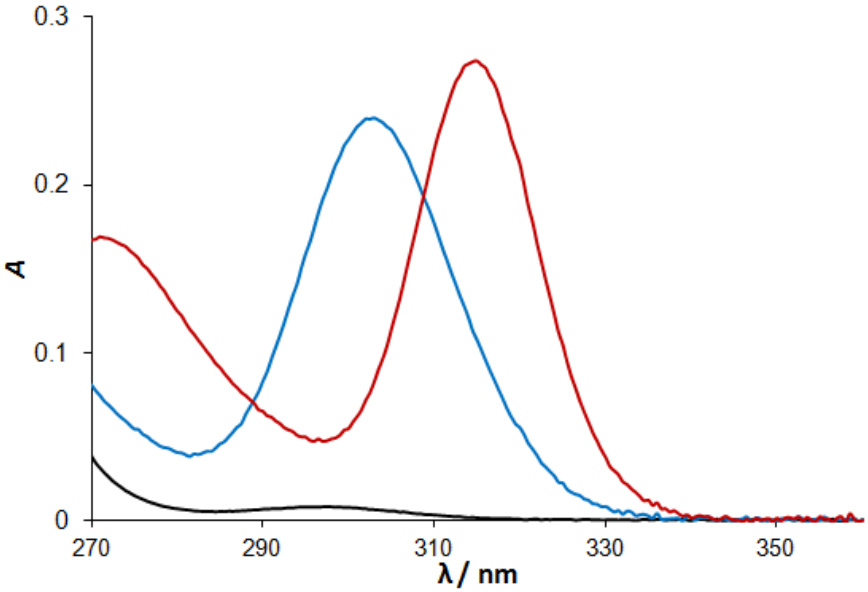

Figure S4. Representative absorption spectra: Ce^{III} aqua ion (black), *out-of-cage* (blue) and *in-cage* (red) Ce^{III}-do3aP^{PIN}complex ($c_M = c_L = 4.0 \cdot 10^{-4}$ M, 25 °C).

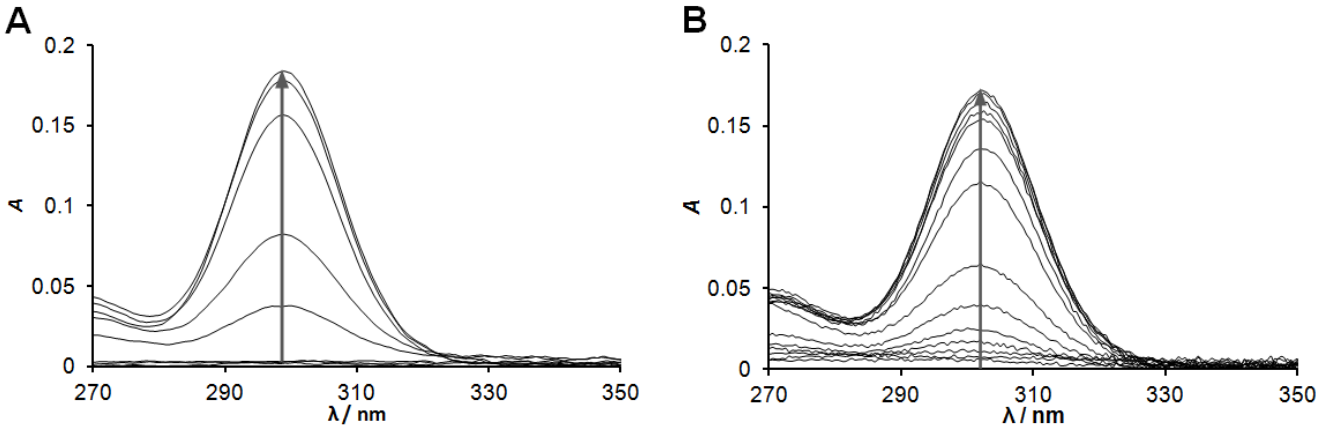

Figure S5. Representative absorption spectra of Ce^{III}–H_4do3aP^H (**A**, pH ~ 1–3) and Ce^{III}–H_5do3aP^{PIN} (**B**, pH ~ 0–3) systems measured immediately after mixing at various pH ($c_M = c_L = 4.0 \cdot 10^{-4}$ M, 25 °C). The arrow indicates increasing pH. Changes of absorbance at absorption band maximum are shown in Figure S6.

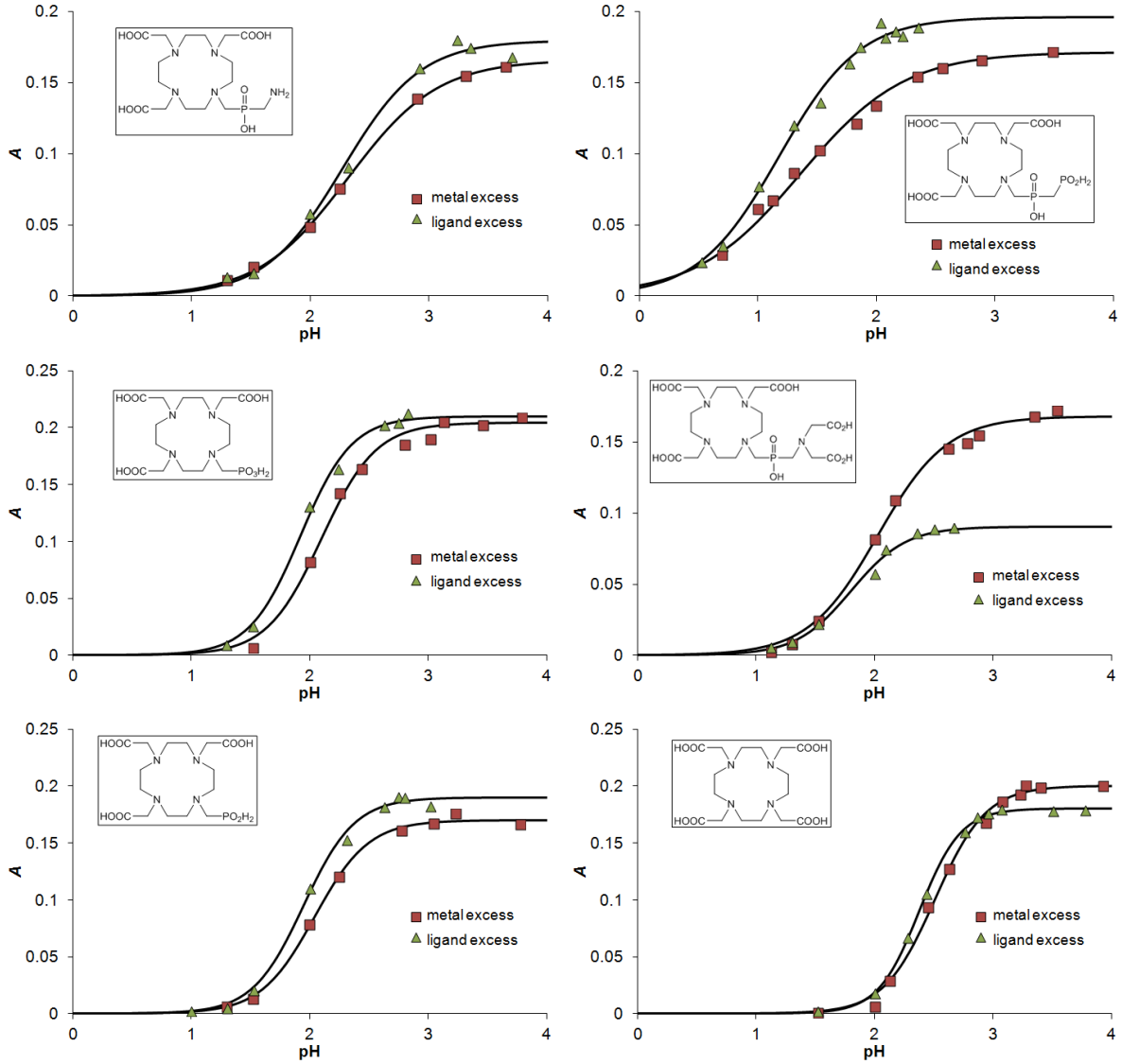

Figure S6. Formation of o*ut-of-cage* complexes: pH dependence of absorbance at absorption band maximum (298–305 nm) measured immediately after mixing of the components (25 °C) under the Ce^{III} excess ($4.0 \cdot 10^{-3}$ M, c_L = $4.0 \cdot 10^{-4}$ M) and under the ligand excess (c_{Ce} = $4.0 \cdot 10^{-4}$ M, c_L = $4.0 \cdot 10^{-3}$ M). The lines correspond to the best fits according to Equation 2.

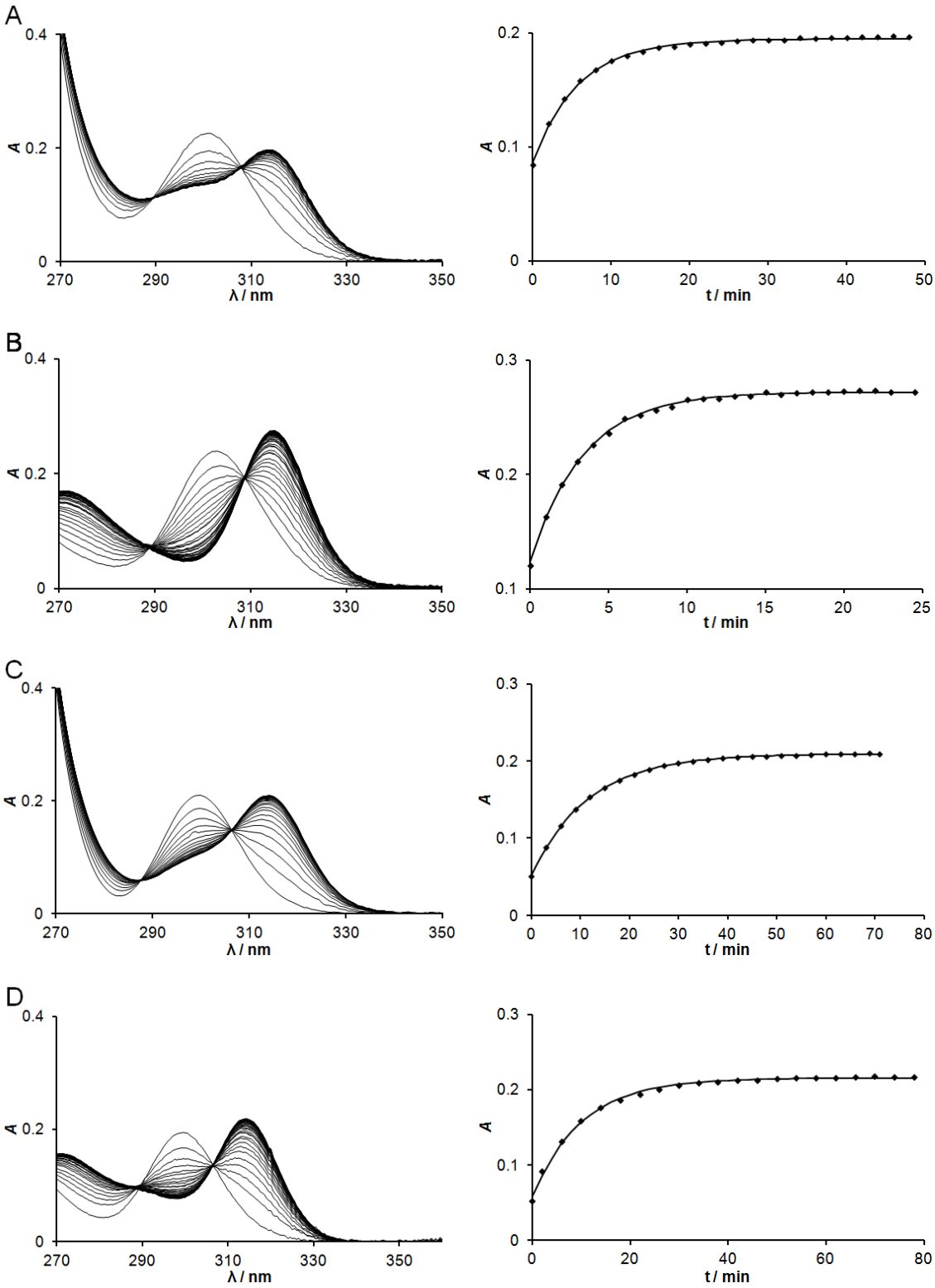

Figure S7. Changes of absorption spectra in the course of complexation of H_5do3aP^{PIN} and H_4do3aP^{AM} (left, 25 °C) and time dependences of absorbance at absorption band maximum (~ 315 nm) of the *in-cage* complex (right). The curves represent the best fit according to Equation 1. **A**: H_5do3aP^{PIN}, $c_{Ce} = 4.0 \cdot 10^{-4}$ M, $c_L = 4.0 \cdot 10^{-3}$ M, pH = 5.4; **B**: H_5do3aP^{PIN}, $c_{Ce} = 4.0 \cdot 10^{-3}$ M, $c_L = 4.0 \cdot 10^{-4}$ M, pH = 5.4; **C**: H_4do3aP^{AM}, $c_{Ce} = 4.0 \cdot 10^{-4}$ M, $c_L = 4.0 \cdot 10^{-3}$ M, pH = 5.7; **D**: H_4do3aP^{AM}, $c_{Ce} = 4.0 \cdot 10^{-3}$ M, $c_L = 4.0 \cdot 10^{-4}$ M, pH = 5.7.

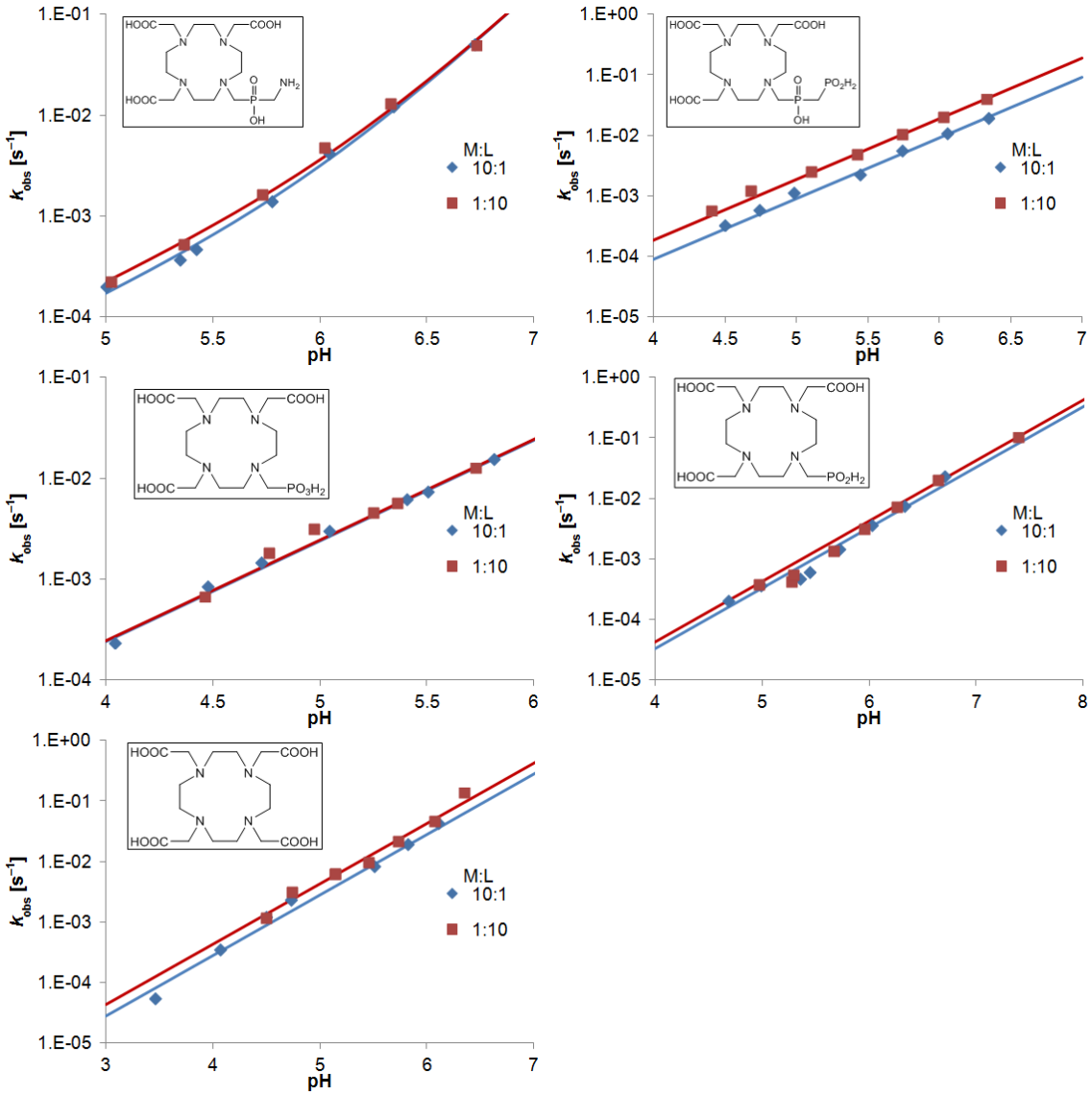

Figure S8. pH dependence of the formation rate constants (25 °C) under the Ce^{III} excess (c_{Ce} = 4.0·10^{-3} M, c_L = 4.0·10^{-4} M, blue diamonds) and under the ligand excess (c_{Ce} = 4.0·10^{-4} M, c_L = 4.0·10^{-3} M, red squares). The lines correspond to the best fits according to Equation 3.